PHYSICAL REVIEW VOLUME 172, NUMBER 3 15 AUGUST 1968

Phase Diagrams of the Cuprous Halides to High Pressures

ELIEZER RAPOPORT AND CARL W. F. T. PISTORIUS
Chemical Physics Group of the National Physical and National Chemical Research Laboratories, South African Council for Scientific and Industrial Research, P. O. Box 395, Pretoria, South Africa

(Received 17 January 1968; revised manuscript received 6 May 1968)

The phase diagrams of CuCl and CuBr to 40 kbar consist of three solid phases and the liquid. One new phase of CuCl, probably disordered bcc, was encountered. The stability region of hexagonal CuBr II is terminated at 6.1 kbar. At higher pressures, there is a direct transition from the zinc-blende structure to disordered bcc. The phase diagram of CuI is complex, with at least seven solid phases, of which five were previously known, below the melting curve to 40 kbar. Hexagonal CuI II cannot exist at higher pressures than 2.2 kbar. The melting curves of the disordered bcc phases of CuCl and CuBr at first rise steeply with pressure, but flatten off considerably above ~25 and ~30 kbar, respectively. This is ascribed to the presence of a denser species in the melt.

INTRODUCTION

THE group-IV elements, such as C (diamond), Si, Ge, and Sn (gray), as well as the III–V and II–VI semiconductors, such as InSb, GaAs, and ZnS, which crystallize with the tetrahedrally coordinated diamond-zinc-blende structure, occupy a central position in solid-state physics and in the physics of high pressures. The bonding is purely covalent in the group-IV elements with this structure, and partially ionic in the related compounds. The percentage ionicity increases as the component elements are further separated in the periodic table. The I–VIII compounds, such as the cuprous and silver halides, are therefore at the extreme ionic end of this sequence. In fact, of the silver halides only AgI belongs to this sequence, since the other silver halides possess the NaCl structure with octahedral coordination.

The phase behavior of the group-IV elements and the III–V and II–VI semiconductors at elevated pressures has been extensively studied, and a recent review[1] collects the data obtained. The phase diagrams appear to follow a prototype diagram in which the solid melts to a denser liquid and therefore yields a falling melting curve. These solids also have high-pressure solid-solid transitions to the white tin or to the NaCl structures, depending on the ionic character of the bonding. The solid-solid transition boundary and the melting curve meet at a triple point, after which the melting curve rises with pressure.

However, the situation is much more complex in the case of AgI and the cuprous halides. AgI has six different solid phases, one of which is metastable, in the pressure range to 100 kbar.[2] Furthermore, the melting curves of both the bcc and NaCl phases are rising,[3] indicating that the liquid is less dense than the corresponding solid. CuCl II (zinc-blende)[4] transforms to CuCl I, which has the hexagonal wurtzite structure, at 407°C.[5] Pure CuCl I melts at 422°C.[6] At high pressures, CuCl II transforms to CuCl IV at a pressure variously given as 42 kbar[7] or 54 kbar.[8] It is possible that this transition may be double,[7] consisting of a rapid one at 42 kbar, followed by a very sluggish transition at 55 kbar. If this is in fact the case, the transition found by Edwards and Drickamer[8] at 54 kbar is almost certainly the same as the 42-kbar transition found by Van Valkenburg[7] and not the same as the 55-kbar transition found by Van Valkenburg. There is yet another transition at ~100 kbar.[8] Jayaraman *et al.*[9] studied CuCl in the region 10–45 kbar by means of differential thermal analysis (DTA) techniques, and followed the II–III transition, however mistaking it for the melting curve. They did not observe the signals corresponding to the actual melting.

At room temperature and pressure, CuBr III has the zinc-blende structure.[4] CuBr III transforms to CuBr II (wurtzite)[10,11] at a temperature in the range 379–400°C.[10–14] The apparently purest samples transform at 385°C.[10,13] CuBr II in turn transforms to CuBr I at 469–470°C.[10,13] The structure of CuBr I is disordered bcc[10,11] as in the case of the high-temperature modification of AgI.[15] The purest CuBr I melts at 483°C.[16] Apparently the presence of small amounts of oxide raises the melting point.[12] The behavior at room temperature and high pressure is not yet quite clear. Van

---

[1] W. Klement, Jr., and A. Jayaraman, Progr. Solid State Chem. 3, 289 (1966).

[2] W. A. Bassett and T. Takahashi, Am. Mineralogist **50**, 1576 (1965).

[3] B. C. Deaton, J. Appl. Phys. **36**, 1500 (1965).

[4] L. Vegard and G. Skofteland, Arch. Math. Naturvidenskab **45**, 163 (1942).

[5] M. R. Lorenz and J. S. Prener, Acta Cryst. **9**, 538 (1956).

[6] R. A. Corley, W. R. Wilcox, and A. B. Chase, Bull. Am. Phys. Soc. **11**, 919 (1966).

[7] A. van Valkenburg, J. Res. Natl. Bur. Std. **68A**, 97 (1964).

[8] A. L. Edwards and H. G. Drickamer, Phys. Rev. **122**, 1149 (1961).

[9] A. Jayaraman, R. C. Newton, and G. C. Kennedy, Proceedings of the International Conference on Industrial Diamonds, Paris, 1962, p. 297 (unpublished).

[10] S. Hoshino, J. Phys. Soc. Japan **7**, 560 (1952).

[11] J. Krug and L. Sieg, Z. Naturforsch. **7A**, 369 (1952).

[12] L. Van My, G. Perinet, and P. Bianco, Bull. Soc. Chim. France **1965**, 3651 (1965).

[13] J. B. Wagner and C. Wagner, J. Chem. Phys. **26**, 1579 (1957).

[14] W. Biermann and H. J. Oel, Z. Physik. Chem. (Frankfurt) **17**, 163 (1958).

[15] L. W. Strock, Z. Physik. Chem. (Leipzig) **B25**, 441 (1934).

[16] N. Sidgwick, *Chemical Elements and Their Compounds* (Oxford University Press, New York, 1950), Vol. I, p. 120.

Valkenburg[7] found two transitions, separated by ~0.1 kbar, at 47 kbar. The phase with the narrow stability range was noncubic, while the higher-pressure form was cubic. In addition there was a transition at 80 kbar to a noncubic form. Edwards and Drickamer[8] found two transitions at ~50 kbar, separated by ~2.5 kbar, and two further transitions at 80 and 95 kbar.

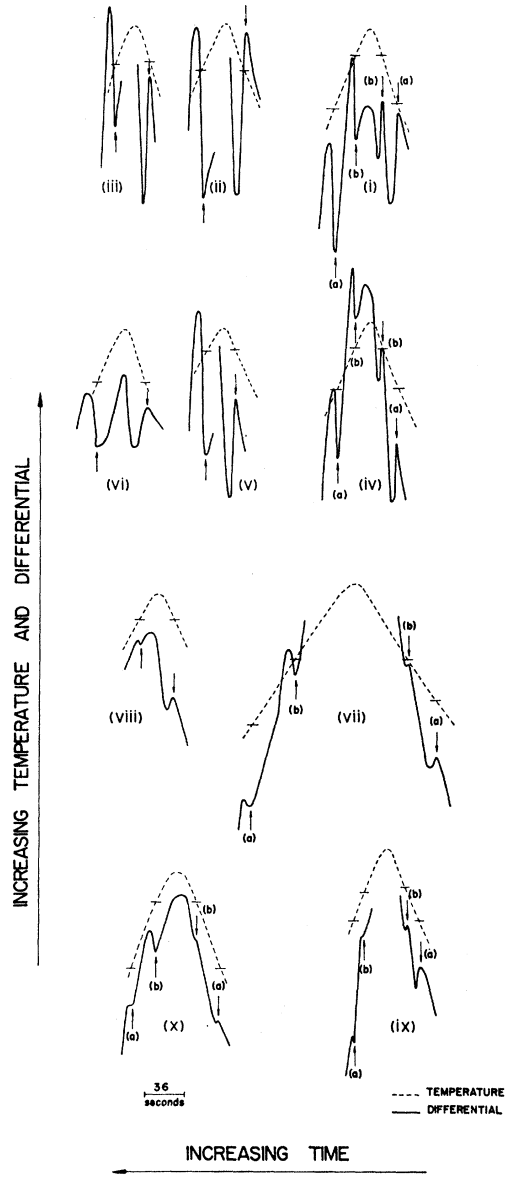

FIG. 1. Typical DTA signals obtained. (i) (a) CuCl II-I at 2.4 kbar. Heating 427°C; cooling 425°C. (b) CuCl I-III at 2.4 kbar. Heating and cooling 446°C. (ii) CuCl II-III at 23.2 kbar. Heating 422.3°C; cooling 421.8°C. (iii) CuCl III melt at 18.6 kbar. Heating 652°C; cooling 649°C. (iv) (a) CuBr III-II at 4.8 kbar. Heating 406.5°C; cooling 406°C. (b) CuBr II-I at 4.8 kbar. Heating and cooling 426°C. (v) CuBr III-I at 9.2 kbar. Heating 405°C; cooling 403.5°C. (vi) CuBr I melt at 11.0 kbar. Heating 721°C; cooling 720°C. (vii) (a) CuI III-II at ~0 kbar. Heating 370.5°C; cooling 360°C. (b) CuI II-I at ~0 kbar. Heating and cooling 408.5°C. (viii) CuI I melt at 3.7 kbar. Heating 722.5°C; cooling 722°C. (ix) (a) CuI I-VII at 8.4 kbar. Heating 786°C; cooling 785.5°C. (b) CuI VII melt at 8.4 kbar. Heating 814°C; cooling 811°C. (x) (a) CuI IV-V at 22.8 kbar. Heating 430.5°C; cooling 429°C. (b) CuI V-VI at 22.8 kbar. Heating and cooling 465°C.

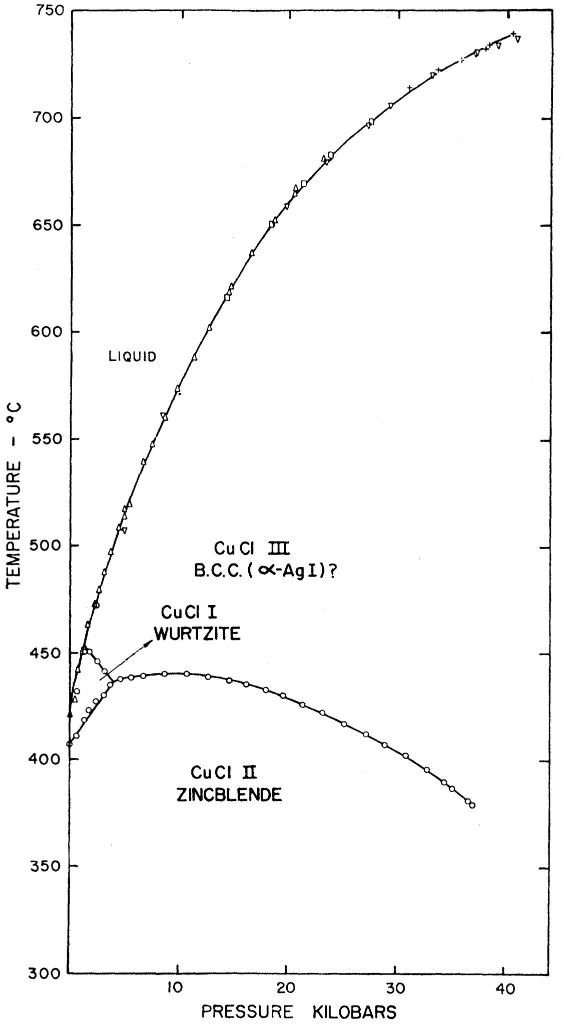

FIG. 2. Phase diagram of CuCl to 40 kbar.

CuI III (zinc-blende[4]) transforms to CuI II (wurtzite[11,17]) at 369°C.[17] CuI II transforms at 407°C[17] to an fcc[11,17] phase, CuI I, which appears to be identical to CuI III except for the presence of considerable positional disorder.[17] CuI I melts at 588–600°C.[12,18] As in the case of CuBr I, one may expect the purest preparation to yield the lower melting point. CuI III compressed at 25°C transforms to CuI IV at 12.9 kbar.[9,19] There are further transitions at 41 and 80 kbar,[8] and transitions at 4 and 5 kbar were observed optically.[7] The extrapolation of the CuI III–IV transition to zero pressure[9]

---

[17] S. Miyake, S. Hoshino, and T. Takenaka, J. Phys. Soc. Japan **7**, 19 (1952).

[18] G. B. Kauffman and R. P. Pinnell, Inorg. Syn. **6**, 3 (1960).

[19] P. W. Bridgman, Proc. Am. Acad. Arts Sci. **76**, 71 (1945) as modified to agree with the more accurate data above 100°C in P. W. Bridgman, Proc. Am. Acad. Arts Sci. **52**, 89 (1916).

TABLE I. Phase behavior of CuCl.

Transition line	Fit (P in kbar)	Standard deviation
CuCl I-III	$t(°\mathrm{C}) = 451 - 5.46\ (P\text{-}1.2)$	0.4°C
CuCl II-I	$t(°\mathrm{C}) = 407 + 8.09\ P$	1.5°C
CuCl II-III	$t(°\mathrm{C}) = 436.5 + 0.786(P\text{-}3.8) - 0.074\ (P\text{-}3.8)^2$	1.0°C
CuCl I-liquid	$P/27.13 = [T(°\mathrm{K})/694]^{1.002} - 1$	3.0°C[a]
CuCl III-liquid	$(P\text{-}1.2)/3.405 = [T(°\mathrm{K})/724]^{7.388} - 1$	6.8°C (Max. dev. 17°C)
	or	
	$t(°\mathrm{C}) = 451 + 17.98(P\text{-}1.2) - 0.43(P\text{-}1.2)^2 + 0.004(P\text{-}1.2)^3$	2.8°C (Max. dev. 5°C)
Triple point	Pressure (kbar)	Temperature (°C)
CuCl I-III-II	3.8	436.5
CuCl III-IV-II	~64	~215
CuCl III-I-liquid	1.2	451

[a] The pressure range is inadequate to yield more than a strictly formal fit.

is not justified in view of the presence of the III–II and II–I transitions.

EXPERIMENTAL

Merck G.R. grade CuCl was used. The stated purity was 99.9%, but the material was slightly green in color because of the presence of a small amount of $CuCl_2$. The substance was therefore purified by dissolving it in concentrated hydrochloric acid and reprecipitating by dilution with distilled water. The pure white precipitate was washed with acetone, dried and stored over P_2O_5. BDH Reagent grade CuBr and CuI with stated purities of 99% were purified in similar ways. The purified material was creamy white in the case of CuBr, and pale flesh colored in the case of CuI.

Pressures up to 40 kbar were generated in a piston-cylinder device.[20] The furnace assembly was similar to that used by Klement *et al.*[21] Phase changes were detected by means of differential thermal analysis, using Chromel-Alumel thermocouples. Corrections were made for the effect of pressure on the thermocouples.[22] The salts were contained in copper capsules which incorporated thermocouple wells.[23] The axial thermal gradient along the sample capsule was reduced by sandwiching the capsule between two insulated copper plugs.[24] Typical DTA signals obtained are shown in Fig. 1. No trace of reaction with the capsule material or of decomposition was observed. Each phase diagram was based on at least six separate runs. The results of different runs were consistent. The heating rate was usually in the range 0.7–2.0°C/sec. Temperatures could be determined to ±1–2°C. Sliding friction was determined by comparing results obtained on increasing and on decreasing pressure. The pressures obtained in this way were further corrected for the effect of nonsymmetrical pressure loss.[25] The procedure based on calibration against the KCl transition[26] at the temperature concerned has been described elsewhere.[25] The corrected pressures are believed accurate to better than ±0.5 kbar. Unless otherwise stated, the points plotted represent the mean of heating and cooling in the case of solid-solid transitions, and the melting signals in the case of solid-liquid phase changes. The techniques used to follow the phase boundaries below ~4 kbar have been described elsewhere.[27]

RESULTS

Cuprous Chloride

The phase diagram of CuCl is shown in Fig. 2. The II-I transition yielded sharp and strong DTA signals, with less than 2°C hysteresis between heating and cooling [Fig. 1(ia)]. Our room-pressure transition temperature was 407±1.5°C in agreement with the literature.[5] The melting curve of CuCl I rises to a triple point CuCl III-I-liquid at 1.2 kbar, 451°C, where a new phase CuCl III appears. The I-III transition yielded sharp DTA signals which were somewhat weaker than those due to the II-I transition [Fig. 1(ib)]. Thermal hysteresis was less than 2°C at heating/cooling rates below 2°C/sec. The CuCl II-I and I-III transition lines meet at a triple point CuCl III-II-I at 3.8 kbar, 436.5°C. The resulting II-III transition yielded very strong and sharp DTA signals [Fig. 1(ii)] with less than 0.5°C thermal hysteresis. The II-III transition line rises gently with pressure, passes through a broad maximum at 9.2 kbar, 439°C, and then falls with increasing pressure. The melting-freezing DTA signals [Fig. 1(iii)]

---

[20] G. C. Kennedy and P. N. La Mori, in *Progress in Very High Pressure Research,* edited by F. P. Bundy, W. R. Hibbard, Jr., and H. M. Strong (John Wiley & Sons, Inc., New York, 1961).

[21] W. Klement, Jr., L. H. Cohen, and G. C. Kennedy, J. Phys. Chem. Solids **27**, 171 (1966).

[22] R. E. Hanneman and H. M. Strong, J. Appl. Phys. **36**, 523 (1965); **37**, 612 (1966).

[23] C. W. F. T. Pistorius, J. Phys. Chem. Solids **26**, 1543 (1965).

[24] E. Rapoport, J. Chem. Phys. **45**, 2721 (1966).

[25] C. W. F. T. Pistorius, E. Rapoport, and J. B. Clark, Rev. Sci. Instr. **38**, 1741 (1967).

[26] C. W. F. T. Pistorius, J. Phys. Chem Solids **25**, 1477 (1964).

[27] C. W. F. T. Pistorius, J. Phys. Chem. Solids **28**, 1811 (1967); E. Rapoport, J. Chem. Phys. **46**, 3279 (1967).

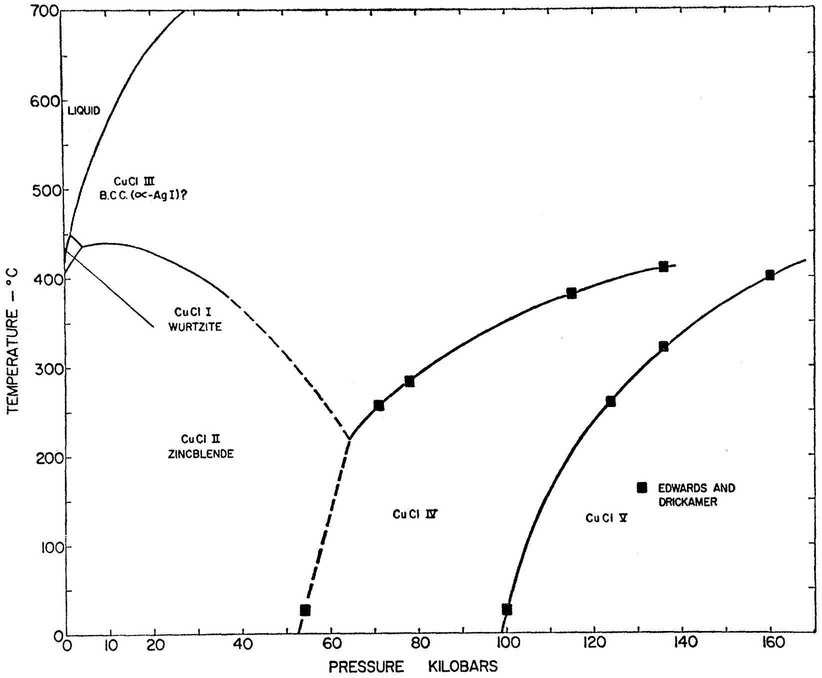

FIG. 3. Proposed phase diagram of CuCl to 170 kbar.

were extremely strong and sharp. The melting curve of CuCl III rises steeply with pressure.

The phase relations of CuCl are summarized in Table I. The polymorphic phase boundaries were fitted to simple power series, and the melting curves to the Simon equation[28]

$$P-P_0=A[(T/T_0)^c-1],$$

where T°K is the melting point at P kbar, P_0 and T_0 are the coordinates of the triple point of the phase in question, and A and c are adjustable constants. A and c were determined by means of Babb's method.[29] However, the fit obtained for the melting curve of CuCl III was poor, giving a standard deviation of 6.8°C, with a maximum deviation of 17°C. The deviations were not random, but showed definite regions where the Simon fit did not agree with the experimental data. An inspection of the melting curve shows that the slope decreases fairly suddenly at ~25 kbar. This is not due to contamination, as was shown by the satisfactory retracing of the melting curve and by the fact that runs in which the first melting point was taken at ~30 kbar yielded results identical to runs where the ~30-kbar point represented the twentieth melting-freezing cycle. Neither is there any evidence for further polymorphism. There seems to be no doubt that this effect is real. An alternative power-series fit, shown in Table I, was satisfactory.

The latent heat of the CuCl II-I transition has apparently not yet been determined. The latent heat of fusion of CuCl I is 2.45–2.62 kcal/mole.[30,31] The initial

TABLE II. Phase behavior of CuBr.

Transition line	Fit (P in kbar)	Standard deviation
III-II	$t(°\mathrm{C})=384.5+4.64\,P$	0.9°C
II-I	$t(°\mathrm{C})=469.5-9.16\,P$	1.1°C
III-I	$t(°\mathrm{C})=413-2.14(P\text{-}6.1)-0.088(P\text{-}6.1)^2$	1.3°C
I-liquid	$P/2.733=[T(°\mathrm{K})/757]^{5.936}-1$	4.5°C
Triple point	Pressure (kbar)	Temperature (°C)
I-III-II	6.1	413
I-IV-III	~51	~100
III-IV-V(?)	~47	~−20

---

[28] F. E. Simon and G. Glatzel, Z. Anorg. Allgem. Chem. **78**, 309 (1929).

[29] S. E. Babb, Jr., Rev. Mod. Phys. **35**, 400 (1963).

[30] K. K. Kelley, U. S. Bur. Mines Bull. **393**, 45 (1936).

[31] A. N. Krestovnikov and G. A. Karetnikov, Zh. Obshch. Khim. **6**, 955 (1936).

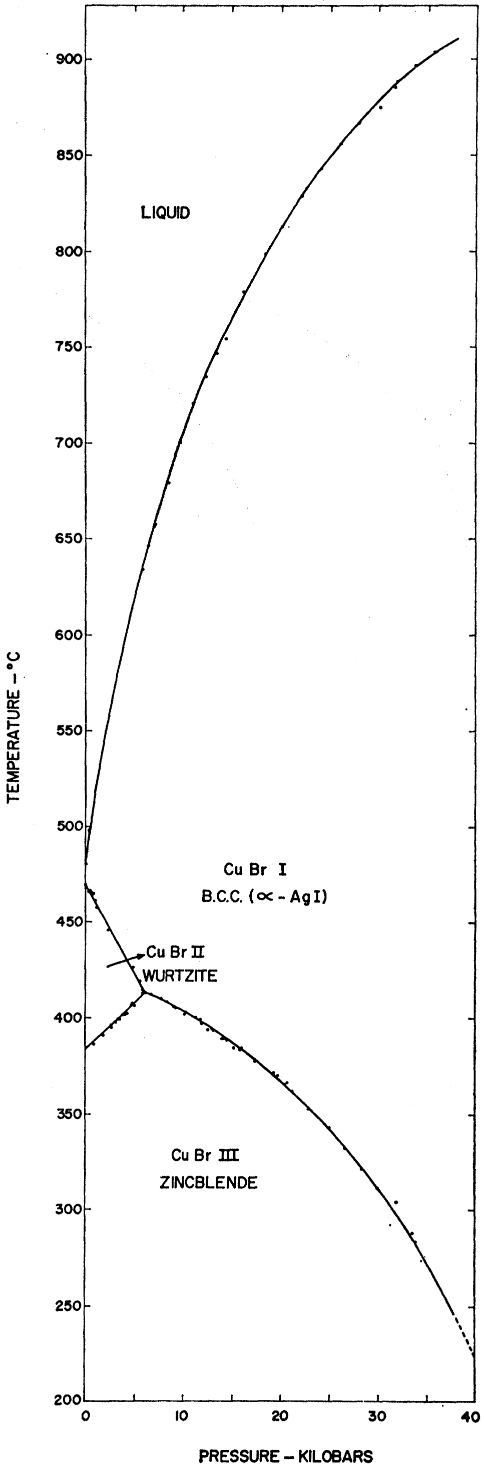

FIG. 4. Phase diagram of CuBr to 40 kbar.

slope of the melting curve is given by

$$(dT/dP)_{P=0} = T_0/Ac = 25.3°\text{C/kbar}$$

by differentiation of the Simon equation. Applying the Clapeyron relation, the volume change on melting of CuCl I is found to be

$$\Delta v_{\text{I-liq}} = 3.7\text{–}4.0 \text{ cm}^3/\text{mole}.$$

Approximate high-temperature trajectories for the high-pressure transitions of CuCl at ~50 and ~100 kbar have been determined by Edwards and Drickamer.[8] The present CuCl II-III phase boundary cannot be made to extrapolate to the room-temperature point of the ~50-kbar transition, and should meet the boundary proposed by Edwards and Drickamer[8] in a triple point CuCl IV-II-III at ~64 kbar, ~215°C. The proposed phase diagram of CuCl to 170 kbar is shown in Fig. 3. The CuCl IV-II-III triple point explains the apparent curvature of the CuCl II-IV transition line found previously.[8]

Cuprous Bromide

The phase diagram of CuBr to 40 kbar is shown in Fig. 4. The III-II and II-I transitions yielded sharp and strong DTA signals, with no observable hysteresis between heating and cooling [Fig. 1(iv)]. Our room-pressure transition temperatures were 384.5±1°C and 469.5±1°C, respectively, in excellent agreement with the literature values for pure samples, viz. 385°C[10,13] and 469–470°C,[10,13] respectively. The III-II transition line rises with pressure, while the II-I transition line falls with pressure and meets the III-II line in a triple

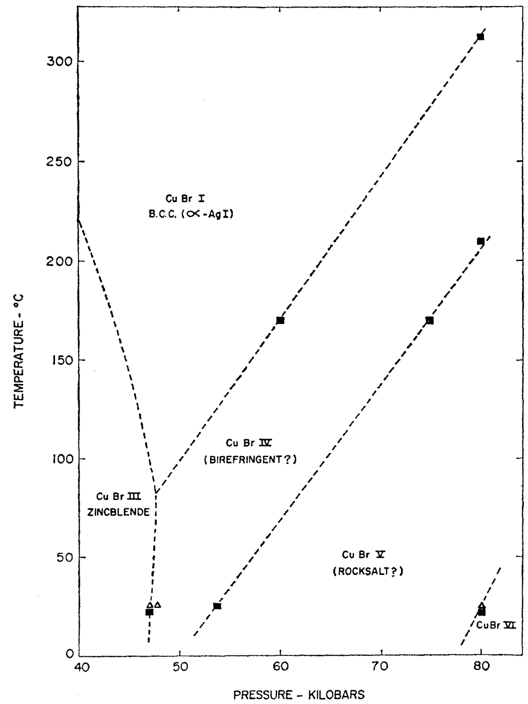

FIG. 5. Proposed phase diagram of CuBr in the range 40–80 kbar. △—Van Valkenburg (1964); ■—Edwards and Drickamer (1961).

point CuBr I-III-II at 6.1 kbar, 413°C. The resulting III-I transition yields very strong DTA signals, with the hysteresis between heating and cooling not exceeding 2°C for heating or cooling rates below 1.5°C/sec [Fig. 1(v)]. The III-I transition line falls with pressure. The melting and freezing DTA signals were somewhat weaker and less sharp than the polymorphic signals [Fig. 1(vi)]. Our room-pressure melting point was located at 484±1°C in good agreement with the literature value, viz., 483°C.[16] The melting curve rises steeply with pressure.

The phase relations of CuBr are summarized in Table II. The latent heats of the III-II and II-I transitions have been determined[10] by means of calorimetric methods, using specific-heat curves, and also from a consideration of DTA peak areas.[12] The two sets of observations differ considerably, but both are in agreement as to the fact that $\Delta H_{\text{III-II}} \simeq 2\Delta H_{\text{II-I}}$. The earlier determination[10] yielded

$$\Delta H_{\text{III-II}} = 1.4 \text{ kcal/mole}$$

and

$$\Delta H_{\text{II-I}} = 0.7 \text{ kcal/mole.}$$

Using the present initial slopes, viz. 4.64°C/kbar and −9.16°C/kbar, respectively, we obtain

$$\Delta v_{\text{III-II}} = +0.41 \text{ cm}^3\text{/mole}$$

and

$$\Delta v_{\text{II-I}} = -0.36 \text{ cm}^3\text{/mole.}$$

The high-temperature x-ray study made by Hoshino[10] was not very accurate, but a similar study by Krug and Sieg[11] was sufficiently accurate to yield significant order-of-magnitude values for the volume changes. Assuming that the thermal expansion coefficient of CuBr III is the same as that[17] of the isostructural CuI III, we obtain

$$\Delta v_{\text{III-II}} \simeq 0.14 \text{ cm}^3\text{/mole}$$

and

$$\Delta v_{\text{II-I}} \simeq -0.06 \text{ cm}^3\text{/mole.}$$

These values are in gross disagreement with the values obtained above using the latent heats determined by Hoshino.[10] However, Van My *et al.*[12] obtained

$$\Delta H_{\text{III-II}} = 0.64 \text{ kcal/mole}$$

and

$$\Delta H_{\text{II-I}} = 0.32 \text{ kcal/mole,}$$

which yield

$$\Delta v_{\text{III-II}} = 0.19 \text{ cm}^3\text{/mole}$$

and

$$\Delta v_{\text{II-I}} = -0.16 \text{ cm}^3\text{/mole.}$$

These values are in good agreement with the x-ray values of Krug and Sieg,[11] and the latent heats of Van My *et al.*[12] can therefore be regarded as approximately correct.

The initial slope of the melting curve is given by $(dT/dP)_{P=0} = T_0/Ac = 46.7$°C/kbar. The latent heat of melting is 1.08 kcal/mole.[12] We then obtain

$$\Delta v_{\text{I-liq}} = 2.78 \text{ cm}^3\text{/mole.}$$

The present CuBr III-I boundary cannot reasonably be made to extrapolate to the point 47–50 kbar, 25°C where the first high-pressure polymorphic transition[7,8] occurs. The transition at 47–50 kbar, 25°C therefore requires a separate phase CuBr IV, and a triple point CuBr I-IV-III, which should be located near 80–120°C, 47–55 kbar. The proposed phase diagram of CuBr in the pressure range 40–85 kbar is shown in Fig. 5. As drawn, the phase diagram implies that the transitions observed by Van Valkenburg[7] at ~47 and ~47.1 kbar correspond with the transitions observed by Edwards and Drickamer[8] just below and just above ~50 kbar, respectively. The CuBr V-VI transition at ~80 kbar[7,8] is from a cubic (possibly NaCl-structure) form to a noncubic form.[7] However, the CuBr VI-VII transition at ~95 kbar[8] (not shown in Fig. 5) may be to a cubic form once again—possibly with the CsCl structure.

Cuprous Iodide

The phase diagram of CuI to 40 kbar is shown in Figs. 6(a) and 6(b), and is considerably more complex than those of CuCl or CuBr. The III-II transition yielded quite small but sharp DTA signals [Fig. 1 (viia)]. The II → III transition temperature depended strongly on the rate of cooling, while the III → II transition temperature was independent of the heating rate. Only the III → II transition temperatures were plotted. The small but sharp signals due to the II-I transition [Fig. 1(viib)] showed no observable hysteresis between heating and cooling. Our room-pressure transition temperatures were 370.5±1°C and 408.5 ±1°C for the III-II and II-I transitions respectively, in good agreement with the literature values 369 and 407°C.[17] The CuI III-II transition line rises with pressure to 2.2 kbar, 374°C, and then sharply changes slope to fall with pressure. The CuI II-I transition line falls with pressure to 2.1 kbar, 403°C, and then also sharply changes slope to rise with pressure. This behavior is clearly due to a polymorphic transition line CuI II-IV which runs nearly vertically between these two triple points, and therefore has a negligible latent heat, but a considerable volume change. No DTA signals due to the II-IV transition were seen or expected.

The DTA signals due to the CuI III-IV transition were similar to those due to the III-II transition, but the thermal hysteresis was usually less than 3°C. The CuI III-IV transition line falls with pressure, and connects smoothly with Bridgman's points[19] at lower temperatures.

The signals due to the IV-I transition were similar to those due to the II-I transition, and also showed no observable hysteresis between heating and cooling. The

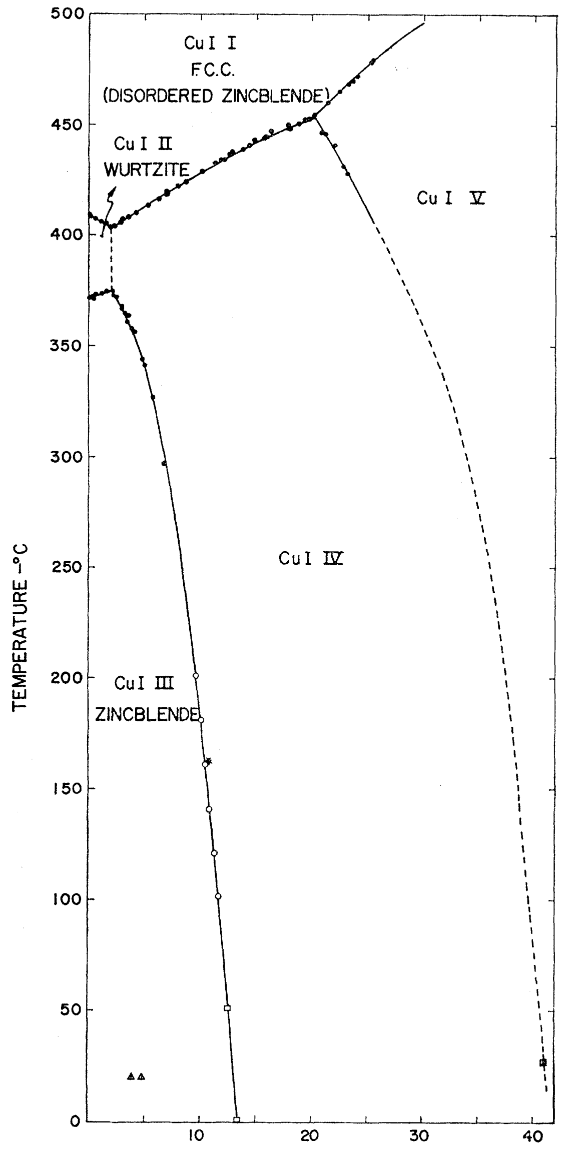

(a)

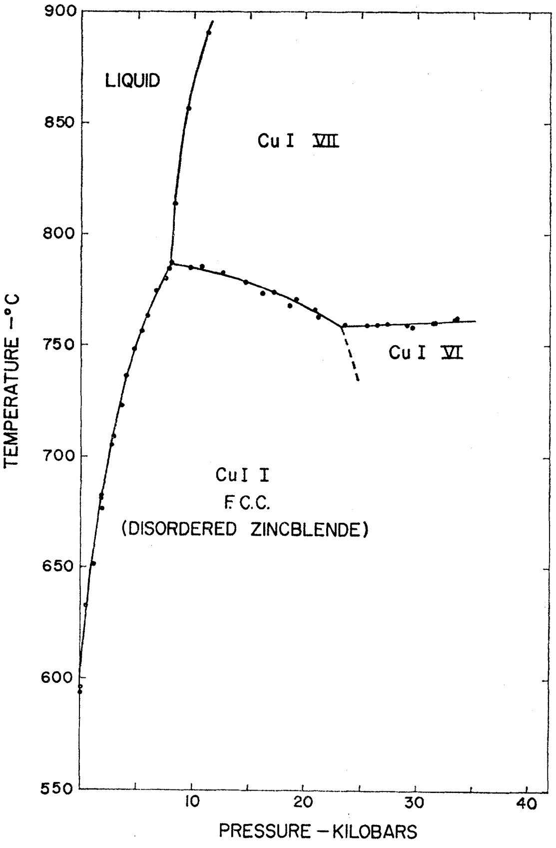

(b)

FIG. 6. (a) The phase diagram of CuI to 42 kbar. The dashed lines indicate suggested phase boundaries. ●—Present work DTA; ○—Bridgman (1916) volumetric; ■—Edwards and Drickamer (1961) optical; □—Bridgman (1937) volumetric, corrected to agree with Bridgman (1916); △—Van Valkenburg (1964) optical; *—Jayaraman *et al.* (1962) volumetric. (b) The high-temperature portion of the phase diagram of CuI to 42 kbar. The dashed line indicates a suggested phase boundary.

IV-I transition line rises with pressure to 20.3 kbar, 453°C, where it splits into two lines with the appearance of CuI V. The IV-V and V-I transitions both yield small but sharp DTA signals [Fig. 1(x)], and show less than 2°C hysteresis between heating and cooling. The IV-V transition line falls with pressure to extrapolate smoothly to the transition point at 41 kbar, 25°C observed by Edwards and Drickamer.[8] This shows that the phase stable at 25°C and pressures above 12.9 kbar[19] is simply CuI IV. It is also probable, in view of the smooth extrapolation of the IV-V transition line to 41 kbar, 25°C, that the phase stable at 25°C, 41–80 kbar is CuI V. If this is not the case, yet another phase would be required with a triple point near ~40 kbar, ~100°C similar to the CuBr I-IV-III triple point. This possibility cannot as yet be ruled out. There are no data on the temperature dependence of the 80-kbar transition.[8] The CuI V-I transition line rises with pressure.

The DTA signals due to the melting of CuI I were quite small but sharp [Fig. 1(viii)]. Our room-pressure melting point was 591±1.5°C in good agreement with the literature value of 588°C.[18] The melting curve of CuI I rises steeply with pressure to a triple point CuI VII-I-liquid at 8.0 kbar, 786.5°C. The DTA signals due to the I-VII transition were considerably stronger than those due to the melting of CuI VII [Fig. 1(ix)]. The melting curve of CuI VII rises extremely steeply

Table III. Phase behavior of CuI

Transition line	Fit (P in kbar)	Standard deviation
III-IV	$t(^\circ\mathrm{C})=374-3.84(P\text{-}2.2)-2.64(P\text{-}2.2)^2$	0.6°C
III-II	$t(^\circ\mathrm{C})=370.5+1.77\ P$	0.6°C
II-I	$t(^\circ C)=408.5-2.46\ P$	0.3°C
II-IV	$P=2.1$	...
IV-I	$t(^\circ\mathrm{C})=403+3.50(P\text{-}2.1)-0.04(P\text{-}2.1)^2$	0.6°C
IV-V	$t(^\circ\mathrm{C})=453-6.61(P\text{-}20.3)-0.679(P\text{-}20.3)^2$	1.2°C
V-I	$t(^\circ\mathrm{C})=453+5.12(P\text{-}20.3)-0.075(P\text{-}20.3)^2$	0.8°C
I-VII	$t(^\circ\mathrm{C})=786.5-0.86(P\text{-}8)-0.064(P\text{-}8)^2$	1.2°C
VI-VII	$t(^\circ\mathrm{C})=758.5+0.24(P\text{-}23.4)$	0.9°C
I-liquid	$P/0.931=[T(^\circ\mathrm{K})/864]^{11.075}-1$	2.9°C[a]
VII-liquid	$(P\text{-}8)/0.686=[T(^\circ\mathrm{K})/1060]^{18.68}-1$	1.0°C[a]
Triple point	Pressure (kbar)	Temperature (°C)
II-IV-III	2.2	374
I-IV-II	2.1	403
I-V-IV	20.3	453
VII-I-liquid	8.0	786.5
VII-VI-I	23.4	758.5

[a] The pressure range is inadequate to yield more than a strictly formal fit.

with pressure, while the I-VII transition line falls with pressure to 23.4 kbar, 758.5°C, where the slope of the transition line changes sharply to continue almost horizontally, but without any noticeable change in the DTA signals. This behavior must be ascribed to the appearance of yet another phase, CuI VI. No DTA signals due to the I-VI transition were observed. This suggests that the I-VI transition is either sluggish, or else carries a very low latent heat, which is in agreement with the lack of difference between the signals obtained for the I-VII and VI-VII transitions. However, the volume change of the I-VI transition may be considerable, judging from the change in slope of the I(VI)-VII transition lines at the suggested VII-VI-I triple point. A triple point CuI VI-V-I can be expected at higher pressures when the V-I and I-VI boundaries meet.

The phase relations of CuI are summarized in Table III. As before, the polymorphic phase boundaries were fitted to simple power series, and the melting curves to the Simon equation.[28] However, especially the melting curve CuI VII is based on so few experimental points that the fit obtained cannot be significant. The latent heats of the III-II and II-I transitions are[12]

$$\Delta H_{\mathrm{III}\text{-}\mathrm{II}}=0.61 \text{ kcal/mole}$$

and

$$\Delta H_{\mathrm{II}\text{-}\mathrm{I}}=0.66 \text{ kcal/mole.}$$

Using the present initial slopes, viz., 1.77 and −2.46°C/kbar, respectively, we obtain

$$\Delta v_{\mathrm{III}\text{-}\mathrm{II}}=0.065 \text{ cm}^3\text{/mole}$$

and

$$\Delta v_{\mathrm{II}\text{-}\mathrm{I}}=-0.095 \text{ cm}^3\text{/mole.}$$

Unfortunately the high-temperature x-ray diffraction studies[11,17] are not sufficiently precise to yield significant values of these very small volume changes for comparison purposes.[32] In particular, the fact that CuI I is denser than CuI II is not predicted, possibly due to the neglect of thermal expansion effects.

The CuI II-IV transition line runs closely vertically, i.e., with little or no latent heat, from 2.2 kbar, 374°C to 2.1 kbar, 403°C. If it is assumed that $\Delta H_{\mathrm{II}\text{-}\mathrm{IV}}$ equals zero, and that the entropies of the CuI III-II and II-I transitions remain unchanged to the triple points, the volume changes corresponding to the III-IV and IV-I transitions near the triple points, and therefore the volume change due to the II-IV transition, can be calculated, using the present initial slopes of the III-IV and IV-I transition lines, viz., −3.84 and 3.50°C/kbar, respectively. We obtain

$$\Delta v_{\mathrm{III}\text{-}\mathrm{IV}}=-0.151 \text{ cm}^3\text{/mole,}$$

$$\Delta v_{\mathrm{II}\text{-}\mathrm{IV}}=-0.216 \text{ cm}^3\text{/mole}$$

and

$$\Delta v_{\mathrm{IV}\text{-}\mathrm{I}}=0.141 \text{ cm}^3\text{/mole,}\quad \Delta v_{\mathrm{II}\text{-}\mathrm{IV}}=-0.236 \text{ cm}^3\text{/mole.}$$

The agreement between the two values of $\Delta v_{\mathrm{II}\text{-}\mathrm{IV}}$ calculated at the two triple points is excellent, and supports the over-all consistency of the various experimental results. However, the latent heats obtained by Miyake *et al.*,[17] viz., 1.7 and 0.77 kcal/mole for the III-II and II-I transitions, respectively, differ grossly from those used above, and do not yield consistent results.

The initial slope of the melting curve of CuI I is 83.8°C/kbar. The latent heat is 0.95 kcal/mole.[12] We

---

[32] There is a misprint in Ref. 17 in this connection. The lattice constants of CuI II (the β form) should read $a=4.31kX$ and $c=7.00kX$.

then obtain

$$\Delta v_{\text{I-liq}} = 3.86 \text{ cm}^3/\text{mole}.$$

This value is not a particularly large one, and the extremely high initial slope is therefore due to the small latent heat of melting. However, the present value of the initial slope may be high due to the small pressure range covered by the melting curve of CuI I, and the resulting large effect of small uncertainties in the pressure.

DISCUSSION

It is clear that the phase diagrams of the cuprous halides are quite complex, especially in the case of CuI, and that they have little superficial resemblance to the simple picture presented by Jayaraman *et al.*[9,33] for group-IV elements, and III–V and II–VI semiconductors. The cuprous halides are considerably more ionic in nature than the substances studied previously,[33] but they do not show the simple behavior of the largely ionic silver halides[2,3] either. However, there are strong analogies between the behavior of AgI[2,3] and that of CuCl and CuBr. Furthermore, the phase diagram of AgI is considerably more complex than the phase diagrams of AgCl and AgBr, and in a similar way the phase diagram of CuI is considerably more complex than the phase diagrams of CuCl or CuBr. This may be due to the large size and high polarizability of the iodide ion, and there is, in addition, evidence for the formation of I_3^- ions in one of the high-pressure phases of AgI.[34] Similar phenomema may occur in some of the high-pressure phases of CuI.

The phase diagrams of CuCl and CuBr are very similar. CuBr III and CuCl II, with the zinc-blende structure, transform at higher temperatures to CuBr II and CuCl I, respectively, with the wurtzite structure. CuBr II then transforms to CuBr I with the α-AgI structure (disordered bcc), and it would seem almost certain that CuCl III also possesses this structure, since the CuBr II-I and CuCl I-III phase boundaries both have negative slopes and are located in similar positions in the phase diagrams. Furthermore, the slope and curvature of the melting curve of CuBr I at pressures above 6 kbar is identical to that of the melting curve of CuCl III at pressures above the CuCl III-I-liquid triple point. The strong flattening of the melting curve of CuCl III above ~25 kbar can also be seen, although not as conclusively, in the melting curve of CuBr I above ~30 kbar. This would imply that the CuBr III-I boundary is similar in nature to the CuCl II-III boundary, which appears probable, and also that CuCl IV may be isostructural with CuBr IV. This is possible, since both appear to be birefringent.[7] However, the correspondence at higher pressures is less clear, with CuBr IV transforming to cubic CuBr V, which in turn transforms to probably noncubic CuBr VI at ~80 kbar, with probably yet another transition at ~95 kbar, while CuCl IV transforms to CuCl V at ~100 kbar without the intervention of other phases. The phase diagram of CuI is quite different from those of CuCl and CuBr. The similarity between the optically[7] observed phase of CuI between 4 and 5 kbar and orthorhombic[3,35] AgI IV is striking. However, this suggests that CuI between 5 and 12.9 kbar may possess the NaCl structure like AgI III,[36] and it is difficult to accept that a phase transition from tetrahedral to octahedral coordination would involve a volume change so small that Bridgman[19] failed to observe it. In our view it is possible that the pressures of the transitions in CuI as obtained by Van Valkenburg[7] may be wrongly calibrated, and that his 15-kbar transition pressure may correspond to the 41-kbar transition,[8] and his transitions at 4 and 5 kbar to the III-IV transition which may split into two at low temperatures with the appearance of a phase highly opaque to visible light as in the case of AgI IV.[2] In that case CuI IV will be cubic just like CuBr V and AgI III.

Melting curve maxima and falling melting curves are now known for a considerable number of substances. Klement[37] has pointed out that in all the known cases of such maxima the solid also exhibits at some higher pressure a solid-solid transition with a large volume change, and he proposed a model in which the existence of two species in the liquid in thermal equilibrium is postulated. The denser species is favored by increasing pressure. This model has been put in a semiquantitative form, and equations for the concentration of the two species as a function of pressure and temperature have been derived.[38] This theory has been successfully applied in analyses of resistivity data and Hall-effect data on Cs[39] and Te.[40] However, even if no maximum appears in the melting curve, it is quite possible that more than one species may occur in the melt, especially if high-pressure polymorphism of the solid is known to occur. It is suggested that the sudden flattening of the melting curve of CuCl III, and to a lesser extent of CuBr I, at ~25 and ~30 kbar, respectively, may be caused by the occurrence in the melt of a denser second species with higher coordination than tetrahedral. If this is indeed the case, one may expect that many more examples of this type of behavior may be encountered as measuring techniques improve, and that it may even be found to be a more or less common occurrence.

The high-temperature phases CuCl III, CuBr I, and CuI I, and possibly also CuI VII, are phases belonging to a family of defect structures. They are characterized by an abnormally high ionic conductivity, comparable with that of a molten salt or an aqueous solution of an

---

[33] A. Jayaraman, W. Klement, Jr., and G. C. Kennedy, Phys. Rev. **130**, 540 (1963); **130**, 2277 (1963).

[34] M. J. Moore and D. W. Skelly, J. Chem. Phys. **46**, 3676 (1967).

[35] B. L. Davis and L. H. Adams, Science **146**, 519 (1964).

[36] R. B. Jacobs, Phys. Rev. **54**, 325 (1938).

[37] W. Klement, Jr. (private communication).

[38] E. Rapoport, J. Chem. Phys. **46**, 2891 (1967).

[39] E. Rapoport, Phys. Rev. Letters **19**, 345 (1967).

[40] E. Rapoport, J. Chem. Phys. **48**, 1433 (1968).

electrolyte.[14,41] The large degree of disorder in these phases results in the entropy of fusion being unusually small. This explains why the initial slopes of the melting curves of especially CuI I, CuI VII, and CuBr I are extremely large, although the volume changes upon fusion are not unusually large. It is obvious that this behavior is not necessarily restricted to the α-AgI structures of CuBr I and CuCl III, but can also apply in the case of the disordered fcc defect structure of CuI I.

---

[41] J. Krogh-Moe, Selected Topics in High-Temperature Chemistry (unpublished).

ACKNOWLEDGMENTS

The authors would like to thank Mrs. Martha C. Pistorius for writing the computer programs used in fitting the data, Dr. G. Gafner and R. J. Murphy for valuable discussions, and J. B. Clark for assistance with much of the experimental work. J. Erasmus and his staff and G. O'Grady and his staff kept the equipment in good repair, and were responsible for the manufacture of the furnace parts. Calculations were carried out on the IBM System 360 of the National Research Institute for Mathematical Sciences.

PHYSICAL REVIEW VOLUME 172, NUMBER 3 15 AUGUST 1968

Vibrational Structures Accompanying the Optic Transitions of Bound Electrons in Crystals*†

E. Mulazzi, G. F. Nardelli, and N. Terzi
Istituto di Fisica dell'Università, and Gruppo Nazionale di Struttura della Materia del Consiglio Nazionale delle Ricerche, Milano, Italy

(Received 14 September 1967; revised manuscript received 22 January 1968)

A description of the phonon processes involved in the optic transitions of a bound electron in crystals is presented, with the specific properties of the electron-phonon interactions considered in detail. The set of forces that the "hole-electron pair" exerts on the surrounding lattice are used as coupling constants, and the projected density of states for the perturbed phonon field is fully explained. The orbit radii for the optic electron are assumed to be of the order of, or smaller than, the lattice parameter, and both dipole-allowed and electric-dipole phonon-forced transitions are considered. Short- and long-range forces are examined. The connection between short-range forces and the stress coefficients of the absorption (emission) band is found. The symmetry properties of the electron wave functions are further taken into account in the analysis of electrostatic types of interactions. It is shown that the electric dipole forces activate essentially the normal modes of the perfect lattice, while the short-range forces activate more easily the possible local and pseudolocal modes. An explanation is also suggested for the intraconfiguration transition of rare-earth ions not activating the pseudolocal modes. The Huang-Rhys parameter is split into local (pseudolocal) and continuum-mode terms. It is shown that the continuum-mode term prescribes how the total intensity of the band is shared among multiple-phonon lines (if present) and broad background absorption. The configuration-diagram description of the many-phonon process is subsequently considered, including the exciton absorption. An interpretation is presented of the Stokes shift between absorption and emission bands: The whole Stokes shift is split into a purely Stokes term and a stored-energy term, the latter being related to the infrared component $\mathbf{P}(\mathbf{r})$ of the polarization field. This purely Stokes term, as well as the phonon contribution to the peak position, is evaluated for the F band, within the linear and quadratic approximations for the electron-phonon interaction. Finally, a qualitative explanation is suggested for the Urbach rule in Perovskite-type crystals.

INTRODUCTION

The absorption (emission) coefficient in the visible and uv region due to the optic transitions of a bound electron in crystals has been the subject of extensive research both from a theoretical[1–4] and from an experimental point of view.[5,6] It seems therefore

---

* This research has been sponsored in part by EOAR under Grants No. 65-05 and No. AF-EOAR 67-8 with the European Office of Aerospace Research, U. S. Air Force.

† A preliminary account of this work was presented at the Conference on Electronic and Ionic Properties of Alkali Halides, Milan, July, 1966 and appeared in *Proceedings of the Conference on Electronic and Ionic Properties of Alkali Halides*, edited by R. Fieschi and G. Spinolo (Gruppo Nazionale di Struttura della Materia, Istituto di Fisica dell'Università, Milan, Italy, 1966).

[1] M. Lax, J. Chem. Phys. **20**, 1752 (1952). The first analysis of the many-phonon process was given by W. E. Lamb, Phys. Rev. **55**, 190 (1939) in connection with neutron scattering.

[2] G. Rickayzen, Proc. Roy. Soc. (London) **A241**, 480 (1957).

[3] Yu. E. Perlin, Usp. Fiz. Nauk **80**, 553 (1964) [English transl.: Soviet Phys.—Usp. **6**, 542 (1964)]; this paper contains extensive references to previous works; D. McCumber, J. Math. Phys. **5**, 221 (1964), **5**, 508 (1964). For the connections with the Mössbauer effect, see, for instance: E. A. Trifonov, Fiz. Tverd. Tela **6**, 462 (1964) [English transl.: Soviet Phys.—Solid State **6**, 366 (1964)]; A. A. Maradudin, P. A. Flinn, and J. M. Radcliffe, Ann. Phys. N. Y. **26**, 81 (1964).

[4] M. H. L. Pryce, in *Phonons in Perfect Lattices and Lattices with Point Imperfections*, edited by R. W. H. Stevenson (Oliver and Boyd, Ltd., Edinburgh, 1966).

[5] D. B. Fitchen, R. H. Silsbee, T. A. Fulton, and E. L. Wolf, Phys. Rev. Letters **11**, 275 (1963); C. B. Pierce, Phys. Rev. **135**, A83 (1964). A. E. Hughes, Proc. Phys. Soc. (London) **87**, 535 (1966). For molecular centers see, for instance, T. Timusk and W. Staude, Phys. Rev. Letters **13**, 373 (1964). These papers represent just a sample.

[6] M. Wagner and W. E. Bron, Phys. Rev. **139**, A223 (1965); **139**, A233 (1965); W. E. Bron, *ibid.* **140**, A2005 (1965).